Journal of Marine Science and Technology

Volume 31 | Issue 3 Article 1

Predefined-time Neural Sliding Mode Control based Trajectory Tracking of Autonomous Surface Vehicle

Han Xue
College of Navigation, Jimei University, Xiamen 361021, Fujian,China, miemie66@jmu.edu.cn

Shulin Li
College of Navigation, Jimei University, Xiamen 361021, Fujian,China

Recommended Citation

Xue, Han and Li, Shulin (2023) "Predefined-time Neural Sliding Mode Control based Trajectory Tracking of Autonomous Surface Vehicle," *Journal of Marine Science and Technology*: Vol. 31: Iss. 3, Article 1.
DOI: 10.51400/2709-6998.2697
Available at: https://jmstt.ntou.edu.tw/journal/vol31/iss3/1

RESEARCH ARTICLE

Predefined-time Neural Sliding Mode Control Based Trajectory Tracking of Autonomous Surface Vehicle

Han Xue*, Shulin Li

College of Navigation, Jimei University, Xiamen 361021, Fujian, China

Abstract

With the progress and development of modern industry, it is urgent to develop a more general and mature predefined time control theory system for uncertain nonlinear systems and apply it to practical engineering systems. Therefore, a novel predefined-time sliding mode control is designed to improve the slow convergence speed of asymptotically convergent controllers and finite-time convergent controllers affected by the initial state of the system. The proposed control approach is proved to converge from the initial value to the balance position using Jensen's inequality and Liapunov theorem. The proposed control method can deal with the ship motion system having six Degree-Of-Freedom (DOF) under external disturbance and parameter uncertainty. Furthermore, there are several application scenarios to simulate the proposed algorithm, such as the ship which is required to achieve ideal control accuracy in a short and fixed time. Alternatively, an unmanned ship is required to arrive at the desired location within the specified time. To sum up, this algorithm can extend some existing theoretical results on finite-time and fixed-time control to the predefined-time case.

Keywords: Predefined-time control, Sliding mode control, Unmanned surface vessel

1. Introduction

1.1. Background and motivation

Most ships and automobiles usually need to meet various convergence time constraints during autonomous driving. The finite-time stability control method helps in developing fast controllers for nonlinear systems and has obvious advantages over the traditional control methods. However, it also suffers from some challenges.

(1) the stable time cannot be predefined in advance;
(2) it is a challenging problem to meet the various requirements of different users.

Meanwhile, practical nonlinear systems need to estimate the system convergence time.

1.2. Related work

Nowadays, motion control of autonomous vehicle systems has become increasingly popular [1−3]. In practical situations, predefined-time convergence has been recently used for improving ship control. For instance, Liang studied the scheduled formation tracking control problem of networked surface vehicles with external interference [4]. Moreover, Souissi developed a method for the parameters system selection to guarantee the convergence of the tracking errors to the origin in a prespecified time [5]. As for Yang, he addressed predefined time formation tracking of networked autonomous surface vehicles [6]. Finally, Wang proposed a predefined time-sliding mode arrival law [7].

Recently, the predefined-time sliding mode has been widely studied. For instance, Mazhar studied

Received 2 February 2023; revised 21 June 2023; accepted 28 June 2023.
Available online 6 October 2023

* Corresponding author.
E-mail address: imlmd@163.com (H. Xue).

https://doi.org/10.51400/2709-6998.2697

the predetermined time convergence for a class of second-order nonlinear systems [8]. In addition, Xu proposed an adaptive sliding mode control scheme with practical predefined time convergence [9]. As for Ju, he designed a high-order predefined time extended state observer [10]. Furthermore, Liang discussed distributed predefined time estimation and local tracking [11]. In addition, Liu proposed the globally predefined time stability [12]. Moreover, Sun studied the predefined time trajectory tracking control of uncertain nonlinear robots [13]. Ferrara used sliding surface switching to ensure convergence in a predetermined time [14] and Huang designed a distributed predefined time fractional sliding mode controller [15]. Moreover, Shao proposed a method for designing a predefined time adaptive sliding mode controller with a specified convergence region [16] and Tang proposed a design scheme of a predefined time controller which could adjust the settlement time arbitrarily and accurately when interference is detected [17]. Added to that, Yu proposed a non-singular fast terminal sliding mode control with a predetermined time [18] and Huang designed a distributed predefined time sliding mode controller [19]. Furthermore, Tao studied the predefined time of multiple Euler-Lagrange systems with dynamic leaders [20] and Ma designed a predefined time barrier function adaptive sliding mode control for disturbed systems [21]. As for Li, he studied the sliding mode control synchronization of chaotic systems based on a predetermined time polynomial function [22] and Liang discussed the predefined time stabilization of Takagi-Sugeno fuzzy systems [23]. Finally, Ni proposed a global adaptive neural network tracking control to realize the tracking error converging in the predetermined time [24].

However, there is still a lot of work to improve the predefined time control, such as dealing with disturbance. Therefore, it is necessary to extend some existing theoretical results, applied to finite-time and fixed-time control, to generate them on the predefined-time case.

1.3. Contributions

The contributions of this word are summarized as follows.

(1) A novel predefined-time sliding mode control is designed;
(2) The control approach is proved to converge from the initial value to a balance position based on Jensen's inequality. It is proved that the system converges from its initial to its balance position;
(3) The proposed control method can deal with ship motion systems having six Degree-Of-Freedom (DOF) exposed to external disturbance and parameter's uncertainty.

2. Preliminaries and problem statement

2.1. System model

The ship's motion is shown in Fig. 1.

Referring to Fig. 1, the following variables are used: η represents the position and attitude of ship, ν is the velocity vector, u indicates the surge velocity, v is the sway velocity, r shows the yaw velocity, x is the surge position, y represents the sway position, and ψ is the yaw angle. Moreover, z indicates the heave position, θ represents the pitch angle, ϕ is the roll angle, and w is the heave velocity. Finally, p represents the roll velocity, q is the pitch velocity, and J indicates the transformation matrix. The six DOF control equations for ships can be represented in the following form [25−28]:

$$\dot{\eta} = J(\eta)\upsilon \tag{1}$$

$$M_1\dot{\upsilon} + C_1\upsilon + D_1\upsilon + g(\eta) + g_0 = \tau + \tau_1 \tag{2}$$

$$\eta = [x, y, z, \phi, \theta, \psi]^T \tag{3}$$

$$\upsilon = [u, v, w, p, q, r]^T \tag{4}$$

where M_1 is the weight inertia and hydrodynamic additional inertia, D_1 represents the linear hydrodynamic damping parameter matrix, and τ is the input force and moment, C_1 indicates the Coriolis and Centripetal torques matrix and τ_1 is the disturbance. Moreover, g is a vector of generalized gravitational and buoyancy forces. The static restoring forces and the moments due to ballast systems and water tanks are collected using the g_0 term.

Furthermore, τ has six components where the attitude is controlled by three horizontal fins, two vertical ones, and the propeller's speed of rotation n.

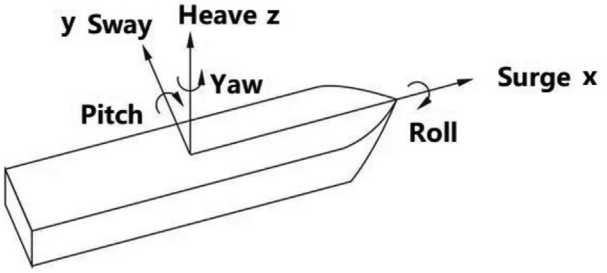

Fig. 1. Model of the ship motion.

In addition, δ_s is the force along the port and starboard stern plane, δ_{bp} represents the force along the port bow plane, δ_{bs} indicates the force along the starboard bow plane, δ_r represents the torque by the top and bottom stern rudder, and δ_b is the torque by the top and bottom bow rudder.

Consider the uncertainty modeling, such as ΔM, ΔC, ΔD.

$$M_1 = M + \Delta M \tag{5}$$

$$C_1 = C + \Delta C \tag{6}$$

$$D_1 = D + \Delta D \tag{7}$$

where M is the nominal weight inertia and hydrodynamic additional inertia, D represents the nominal linear hydrodynamic damping parameter matrix, and C shows the nominal Coriolis and Centripetal torques matrix. Thus, Eq. (2) can be rewritten as shown below:

$$M\dot{\upsilon} + C\upsilon + D\upsilon = \tau + \tau_d \tag{8}$$

where τ_d is the uncertain model and disturbance, and

$$\tau_d = d - \Delta M\dot{\upsilon} - \Delta C\upsilon - \Delta D\upsilon - g(\eta) - g_0 \tag{9}$$

2.2. Predefined-time stable

Lemma 1 [29,30]. If there exists a continuous radially unbounded function V satisfying the following constraint:

$$\dot{x} = f(x) \tag{10}$$

$$V(0) = 0 \tag{11}$$

$$V(x) > 0, \forall x \neq 0 \tag{12}$$

and the derivative of V along the trajectories of the system, expressed by Eq. (10), satisfies the following:

$$\dot{V} \leq -\frac{\alpha}{m} e^{\beta V m} V^{1-m} \tag{13}$$

where $0 < m \leq 1$, $\alpha > 0$, $\beta > 0$, then the origin is globally predefined-time stable for the system expressed by Eq. (10) where $T \leq \frac{1}{\alpha\beta}$.

3. Main results

The algorithm targets the trajectory tracking control method for a ship and it comprises the following steps.

1. Obtaining the motion reference of the ship;
2. Building the ship motion model. The motion data is used to adjust the ship's state whereas the input adjustment data is generated according to the comparison result;
3. Calculating the offset between the ship motion data and the motion reference. The motion adjustment data is generated according to the comparative results of the deviation.

Assumption 1. The disturbances and the model unknown items are bounded.

3.1. Predefined-time control strategy

Taking the time derivative of Eq. (1) results in the following:

$$\ddot{\eta} = \dot{J}\upsilon + J\dot{\upsilon} \tag{14}$$

Referring to Eqs. (1) and (14), one can get:

$$\upsilon = J^{-1}\dot{\eta} \tag{15}$$

and

$$\dot{\upsilon} = J^{-1}(\ddot{\eta} - \dot{J}\upsilon) \tag{16}$$

Therefore, substituting Eqs. (15) and (16) into Eq. (8) results in the following:

$$\begin{aligned} &MJ^{-1}\left(\ddot{\eta} - \dot{J}J^{-1}\dot{\eta}\right) + CJ^{-1}\dot{\eta} + DJ^{-1}\dot{\eta} \\ &= MJ^{-1}\ddot{\eta} + \left(CJ^{-1} + DJ^{-1} - MJ^{-1}\dot{J}J^{-1}\right)\dot{\eta} \\ &= \tau + \tau_d \end{aligned} \tag{17}$$

Moreover, denote η_d and $\tilde{\eta}$ as the desired trajectory and the tracking error of the trajectory, respectively, one can write:

$$\tilde{\eta} = \eta - \eta_d \tag{18}$$

Thus, the sliding mode surface can be represented as follows:

$$s = \dot{\tilde{\eta}} + \frac{\tilde{\eta}}{aT\|\tilde{\eta}\|^a} e^{\|\tilde{\eta}\|^a} \tag{19}$$

where $0 < a \leq 1$.

Taking the time derivative of Eq. (19) results in:

$$\dot{s} = \left(a\frac{\tilde{\eta}\tilde{\eta}^T}{\|\tilde{\eta}\|^2} + \left(I - a\frac{\tilde{\eta}\tilde{\eta}^T}{\|\tilde{\eta}\|^2}\right)\frac{1}{\|\tilde{\eta}\|^a}\right)\frac{1}{abT} e^{\|\tilde{\eta}\|^a}\dot{\tilde{\eta}} + \ddot{\tilde{\eta}} \tag{20}$$

Furthermore, denote the sum of estimated disturbance and the uncertain model of τ_d as $\hat{\tau}_d$. The control input is represented as follows:

$$\tau = \left(CJ^{-1} + DJ^{-1} - MJ^T\dot{J}J^{-1}\right)\dot{\eta} + MJ^{-1}\ddot{\eta}_d - MJ^{-1}k\mathrm{sgn}(s) - MJ^{-1}\left(a\frac{\tilde{\eta}\tilde{\eta}^T}{\|\tilde{\eta}\|^2} + \left(I - a\frac{\tilde{\eta}\tilde{\eta}^T}{\|\tilde{\eta}\|^2}\right)\frac{1}{\|\tilde{\eta}\|^a}\right)\frac{1}{aT}e^{\|\tilde{\eta}\|^a}\dot{\tilde{\eta}} - \hat{\tau}_d$$
$$- MJ^{-1}\frac{s}{cdT_2\|s\|^{cd}}e^{\|s\|^{cd}} = \left(C + D - MJ^{-1}\dot{J}\right)J^{-1}\dot{\eta} + MJ^{-1}\ddot{\eta}_d - MJ^{-1}k\mathrm{sgn}(s) -$$
$$MJ^{-1}\left(\frac{\tilde{\eta}\tilde{\eta}^T}{\|\tilde{\eta}\|^2} + \frac{|\tilde{\eta}\|^2 I - a\tilde{\eta}\tilde{\eta}^T}{a\|\tilde{\eta}\|^2\|\tilde{\eta}\|^a}\right)\frac{e^{\|\tilde{\eta}\|^a}\dot{\tilde{\eta}}}{T} - \hat{\tau}_d - \frac{MJ^{-1}se^{\|s\|^{cd}}}{cdT_2\|s\|^{cd}} \tag{21}$$

where k is the gain, the exponent $c \geq 1$, $0<d \leq c^{-1}$, and I is an three-dimensional identity matrix.

3.2. Neural network

Given the presence of external disturbances and parameter variations in an uncertain ship environment, a Neural Network (NN) is employed to approximate the uncertain model. The NN architecture is shown in Fig. 2.

Concerning τ_d, it is computed by the neural network using the below equation:

$$\tau_d = W^T h + \varepsilon \tag{22}$$

where W is the weight matrix. ε is the approximation error of the neural network, and

$$||\varepsilon|| < k \tag{23}$$

Moreover, h represents the Radial basis function which is expressed as follows:

$$h(z) = e^{-\frac{(z-\mu)^T(z-\mu)}{2\sigma^2}} \tag{24}$$

where z is input, μ is the center vector of hidden layer neurons, and σ is the width of the radial basis function.

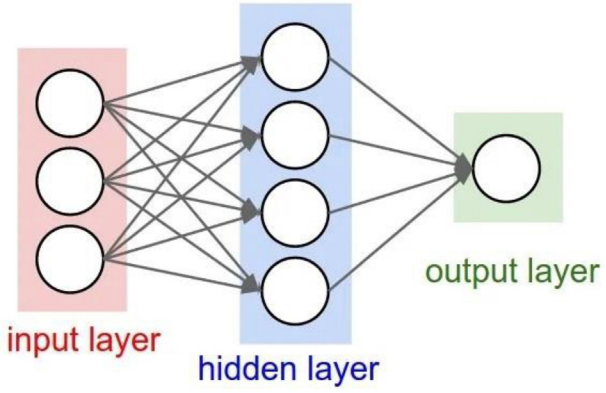

Fig. 2. Structure of the neural network.

The estimated value of τ_d is computed as follows:

$$\tau_d = \hat{\tau}_d + \tilde{\tau}_d \tag{25}$$

where $\tilde{\tau}_d$ is the estimation error of τ_d.

Furthermore, the weight of the NN is composed as follows:

$$W = \widehat{W} + \tilde{W} \tag{26}$$

Finally, $\hat{\tau}_d$ is computed using the NN as follows:

$$\hat{\tau}_d = \widehat{W}^T h \tag{27}$$

Subtracting Eq. (27) from Eq. (23) results in:

$$\tilde{\tau}_d = \tilde{W}^T h + \varepsilon \tag{28}$$

where ε is the approaching error.

The adaptive law of the estimated NN weight is designed as follows:

$$\dot{\widehat{W}} = -\frac{1}{2}c\|s\|^{c-2}s^T h + \frac{1}{2dT_2}\frac{\tilde{W}^T}{\tilde{W}^T\tilde{W}}\left(\tilde{W}^T\tilde{W}\right)^{1-d}e^{\left(\tilde{W}^T\tilde{W}\right)^d} \tag{29}$$

where the coefficient T_2 must be strictly positive.

It can be proven that a NN can obtain a certain solution when the number of iterations approaches infinity, which satisfies the Lipschitz condition. In this case, with a complete norm and Lipschitz constant, the NN is convergent. In fact, the convergence can be described as follows: *given a maximum number of iterations and an error limit, each step of the weight correction in the back-propagation algorithm will reduce its approaching error, and the component of the weight vector will move along the direction of the gradient reduction.* In theory, convergence occurs when the sample size is large enough and the number of iteration steps is enough. In fact, it is possible that, when the iteration reaches a certain number, the approaching error would be smaller than the error limit. Thus, the weight vector meets the requirements and the network training is successful.

Moreover, the gradient limits can be also used as a condition for iteration termination. In this case, convergence means that the gradient update amount is less than a certain value after a certain iteration number. Hence, the weight vector that meets the convergence requirements is obtained.

3.3. Convergence proof

Lemma 2 (Jensen's inequality). For a convex function, the following inequality is satisfied:

$$\frac{\sum_{i=1}^{n} f(x_i)}{n} \geq f\left(\frac{\sum_{i=1}^{n} x_i}{n}\right) \tag{30}$$

Lemma 3. If f is twice continuously differentiable and always positive ($\frac{\partial^2 f}{\partial x^2} \geq 0$), then $f(x)$ is a convex function.

Lemma 4. If $f_1(x)$ and $f_2(x)$ are both twice continuously differentiable, and the following inequalities are satisfied (refer to Eq. (31)).

$$f_1''(x) \geq 0, f_1'(x) \geq 0, f_1(x) \geq 0, f_2''(x) \geq 0, f_2'(x) \geq 0, f_2(x) \geq 0 \tag{31}$$

then $f_1(x) \cdot f_2(x)$ is a convex function.

Proof. The second derivative of $f_1(x)f_2(x)$ is

$$\begin{aligned}\frac{\partial^2(f_1 f_2)}{\partial x^2} &= \frac{\partial}{\partial x}\left(\frac{\partial(f_1 f_2)}{\partial x}\right) = \frac{\partial}{\partial x}(f_1' f_2 + f_1 f_2') \\ &= f_1'' f_2 + f_1' f_2' + f_1' f_2' + f_1 f_2'' = f_1'' f_2 + 2 f_1' f_2' + f_1 f_2''\end{aligned} \tag{32}$$

From Eq. (31), we get:

$$\frac{\partial^2(f_1 f_2)}{\partial x^2} \geq 0 \tag{33}$$

Therefore, according to Lemma 2, $f_1(x)f_2(x)$ is a convex function.

Theorem 2. For the nonlinear kinematics and dynamics equations of the ship, the control law is designed according to Eq. (21). Therefore, the error will converge to the origin within a predetermined time.

Proof: The Lyapunov function is defined as follows:

$$V = \|s\|^c + \tilde{W}^T \tilde{W} \tag{34}$$

Taking the time derivative of Eq. (34) results in obtaining the derivative of Eq. (34):

$$\dot{V} = c\|s\|^{c-2} s^T \dot{s} + 2\tilde{W}^T \dot{\tilde{W}} \tag{35}$$

Substituting Eq. (20) into Eq. (35) results in the following:

$$\dot{V} = c\|s\|^{c-2} s^T \left(\left(a\frac{\tilde{\eta}\tilde{\eta}^T}{\|\tilde{\eta}\|^2} + \left(I - a\frac{\tilde{\eta}\tilde{\eta}^T}{\|\tilde{\eta}\|^2}\right)\frac{1}{\|\tilde{\eta}\|^a}\right)\frac{1}{aT} e^{\|\tilde{\eta}\|^a}\dot{\tilde{\eta}} + \ddot{\tilde{\eta}}\right) + 2\tilde{W}^T \dot{\tilde{W}} \tag{36}$$

In addition, substituting Eq. (17) into Eq. (36) leads to:

$$\begin{aligned}\dot{V} = c\|S\|^{c-2} S^T \Bigg(&\left(\frac{a\tilde{\eta}\tilde{\eta}^T}{\|\tilde{\eta}\|^2} + \left(I - a\frac{\tilde{\eta}\tilde{\eta}^T}{\|\tilde{\eta}\|^2}\right)\frac{1}{\|\tilde{\eta}\|^a}\right)\frac{e\|\tilde{\eta}\|^a \dot{\tilde{\eta}}}{aT} \\ &+ \left(MR^{-1}\right)^{-1}\left(\tau + \tau_d - \left(CR^T + DR^T - MR^T \dot{R} R^T\right)\dot{\eta}\right)\Bigg) \\ &+ 2\tilde{W}^T \dot{\tilde{W}}\end{aligned} \tag{37}$$

Substituting Eq. (21) into Eq. (37) results in:

$$\dot{V} = -c\|s\|^{c-2} s^T \left(k\,\mathrm{sgn}(s) + \frac{s e^{\|s\|^{cd}}}{cdT_2\|s\|^{cd}} - \tilde{\tau}_d\right) + 2\tilde{W}^T \dot{\tilde{W}} \tag{38}$$

Finally, substituting Eq. (29) into Eq. (38) yields in:

$$\begin{aligned}\dot{V} &= -c\|s\|^{c-2} s^T \left(k\,\mathrm{sgn}(s) + \frac{s e^{\|s\|^{cd}}}{cdT_2\|s\|^{cd}} - \varepsilon\right) \\ &\quad - \frac{1}{dT_2}\left(\tilde{W}^T\tilde{W}\right)^{1-d} e^{\left(\tilde{W}^T\tilde{W}\right)^d} \\ &\leq -c\|s\|^{c-2}\left(k\|s^T\| + \frac{\|s\|^{2-cd} e^{\|s\|^{cd}}}{cdT_2} - \|s^T\varepsilon\|\right) \\ &\quad - \frac{1}{dT_2}\left(\tilde{W}^T\tilde{W}\right)^{1-d} e^{\left(\tilde{W}^T\tilde{W}\right)^d}\end{aligned} \tag{39}$$

According to Cauchy-Schwarz inequality, the inequality presented in Eq. (39) is written as follows:

$$\begin{aligned}\dot{V} \leq &-c\|s\|^{c-2}\left(\|s^T\|(k - \|\varepsilon\|) + \frac{\|s\|^{2-cd} e^{\|s\|^{cd}}}{cdT_2}\right) \\ &- \frac{1}{dT_2}\left(\tilde{W}^T\tilde{W}\right)^{1-d} e^{\left(\tilde{W}^T\tilde{W}\right)^d}\end{aligned} \tag{40}$$

Since $||\varepsilon|| < k$, the inequality of Eq. (40) can be written as follows:

$$\begin{aligned}\dot{V} &\leq -\|S\|^{c-2}\frac{\|S\|^{2-cd} e^{\|S\|^{cd}}}{dT_2} - \frac{1}{dT_2}\left(\tilde{W}^T\tilde{W}\right)^{1-d} e^{\left(\tilde{W}^T\tilde{W}\right)^d} \\ &= -\frac{1}{dT_2}\left(\|S\|^c\right)^{1-d} e^{\|S\|^{cd}} - \frac{1}{dT_2}\left(\tilde{W}^T\tilde{W}\right)^{1-d} e^{\left(\tilde{W}^T\tilde{W}\right)^d} \\ &= -\frac{1}{dT_2}\left(\left(\|S\|^c\right)^{1-d} e^{\|S\|^{cd}} + \left(\tilde{W}^T\tilde{W}\right)^{1-d} e^{\left(\tilde{W}^T\tilde{W}\right)^d}\right)\end{aligned} \tag{41}$$

Since $e^{x^d} \geq 0$, $\frac{\partial e^{x^d}}{\partial x} = e^{x^d} d x^{d-1} \geq 0$,

$\frac{\partial^2 e^{x^d}}{\partial x^2} = \frac{\partial(e^{x^d} d x^{d-1})}{\partial x} = e^{x^d} d(x^{d-1} d x^{d-1} + (d-1)x^{d-2}) \geq 0$,

$x^{1-d} \geq 0$, $\frac{\partial x^{1-d}}{\partial x} = (1-d)x^{-d} \geq 0$,

and $\frac{\partial^2 (x^{1-d})}{\partial x^2} = \frac{\partial((1-d)x^{-d})}{\partial x} = -d(1-d)x^{-d-1} \geq 0$,

therefore, according to Lemma 4, $x^{1-d} e^{x^d}$ is a convex function.

Moreover, according to Lemma 2 using Jensen's inequality, one can write:

$$\begin{aligned}\dot{V} &\leq -\frac{2}{dT_2}\left(\frac{1}{2}(\|S\|^c)^{1-d} e^{\|S\|^{cd}} + \frac{1}{2}(\tilde{W}^T\tilde{W})^{1-d} e^{(\tilde{W}^T\tilde{W})^d}\right) \\ &\leq -\frac{2}{dT_2}\left(\frac{\|S\|^c + \tilde{W}^T\tilde{W}}{2}\right)^{1-d} e^{\left(\frac{\|S\|^c + \tilde{W}^T\tilde{W}}{2}\right)^2} \\ &= -\frac{2^d}{dT_2}(\|S\|^c + \tilde{W}^T\tilde{W})^{1-d} e^{2^{-d}(\|S\|^c + \tilde{W}^T\tilde{W})^d} \\ &= -\frac{2^d}{dT_2} V^{1-d} e^{2^{-d} V^d}\end{aligned} \tag{42}$$

In addition, according to Lemma 1, the system error state will converge to zero within time $T \leq \frac{1}{\frac{2^d}{T_2}2^{-d}} = T_2$. Thus, the tracking error of the ship system can reach the expected objective stably within the preset time of the user. Finally, the controller ensures the predefined-time tracking performance.

4. Case studies

4.1. System an results

An autonomous vehicle model is used for testing [31]. Therefore, a simulation experiment has been used.

The initial state of the system is $\eta_0 = [10\text{ m}, 30\text{ m}, -3\text{ m}, 0^o, 0^o, 0^o]^T$ and $\nu_0 = [0\text{ m/s}, 0\text{ m/s}, 0\text{ m/s}, 0^o/s, 0^o/s, 0^o/s]^T$. In addition, the current speed is 0.5 m/s whereas the current direction is 30^o. The main parameters are given below.

The weight inertia and hydrodynamic additional inertia is:

$$M = \begin{bmatrix} 6020.3 & 0 & 0 & 0 & 332.7269 & 0 \\ 0 & 9548.7 & 0 & -380.0698 & 0 & -473.4289 \\ 0 & 0 & 23320 & 0 & 2682.8 & 0 \\ 0 & -380.0698 & 0 & 4129.0 & 13.58 & 84.6732 \\ 332.7269 & 0 & 2682.8 & 13.58 & 49134 & -13.58 \\ 0 & -473.4289 & 0 & 84.6732 & 13.58 & 20696 \end{bmatrix}.$$

As for the linear hydrodynamic damping parameter matrix, is it expressed as follows:

$$D = \begin{bmatrix} 0.5434 & 0 & 0 & 0 & 0 & 0 \\ 0 & 1436.5 & 0 & 0 & 0 & 0 \\ 0 & 0 & 4213.8 & 0 & 0 & 0 \\ 0 & 0 & 0 & 4339.8 & 0 & 0 \\ 0 & 0 & 0 & 0 & 26829 & 0 \\ 0 & 0 & 0 & 0 & 0 & 6313.5 \end{bmatrix}.$$

Moreover, the Coriolis and Centripetal torques matrix is:

$$C = \begin{bmatrix} 0 & 0 & 0 & 1.0541 & 6.4737 & 11.9362 \\ 0 & 0 & 0 & -6.4737 & 1.0541 & -85.9782 \\ 0 & 0 & 0 & -12.1241 & 88.1113 & 0 \\ -1.0541 & 6.4737 & 12.1241 & 0 & 15.7173 & -138.4340 \\ -6.4737 & -1.0541 & -88.1113 & -15.7173 & 0 & -0.7677 \\ -11.9362 & 85.9782 & 0 & 138.4340 & 0.7677 & 0 \end{bmatrix}.$$

Finally, the transformation matrix is defined as follows:

$$J = \begin{bmatrix} 0.9052 & -0.4221 & -0.0501 & 0 & 0 & 0 \\ 0.4214 & 0.9065 & -0.0239 & 0 & 0 & 0 \\ 0.0555 & 0.00055 & 0.9985 & 0 & 0 & 0 \\ 0 & 0 & 0 & 1 & -0.00003 & -0.0556 \\ 0 & 0 & 0 & 0 & 1 & -0.00055 \\ 0 & 0 & 0 & 0 & 0.00055 & 1.0015 \end{bmatrix}.$$

The tracking trajectory is shown in Fig. 3.

The surge position, the sway position, and the heave position are shown in Fig. 4.

Concerning the roll angle, the pitch angle, and the yaw angle, they are presented using Fig. 5.

The surge velocity, sway velocity and heave velocity are shown in Fig. 6.

Finally, the roll angle velocity, pitch angle velocity and yaw angle velocity are shown in Fig. 7.

The input force along the port and the starboard stern plane are shown in Fig. 8.

Moreover, the forces along the port bow plane are shown in Fig. 9.

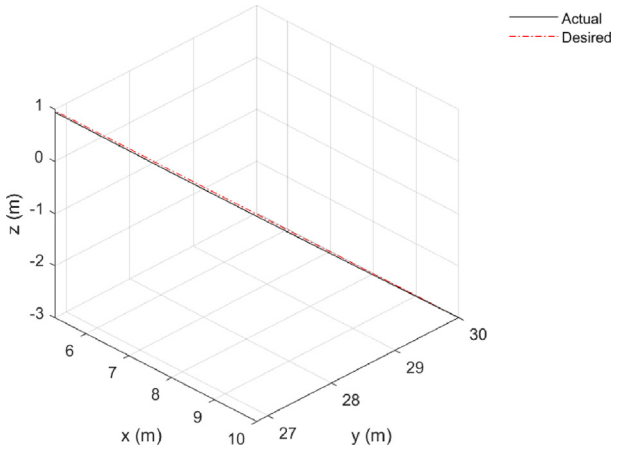

Fig. 3. Tracking trajectory.

As for the torque by the top and bottom stern rudder, they are shown in Fig. 10.

In addition, the torques by the top and bottom bow rudder are shown in Fig. 11.

Finally, the rotation speed of the propeller is shown in Fig. 12.

From the above figures, the ship can fully and stably follow the predefined trajectory. It is illustrated, from Figs. 3–12, that the system can deal with known disturbances. Moreover, the new algorithm can ensure the safe navigation and perform a good tracking of the route under wind and current disturbance due to random sea conditions.

4.2. Performance comparison

To further test the proposed algorithm, it is compared to the finite-time convergence algorithm [32]. Thus, the comparison of control input δ_s, regarding both techniques, is shown in Fig. 13.

Finally, the comparison of control input signals δ_{bp} is shown in Fig. 14.

It is illustrated in Figs. 13 and 14 that, compared to the finite-time algorithm, this proposed algorithm achieves high precision and high speed. Moreover, it is smoother and less chattering than the finite-time control algorithm and it can improve the convergence speed, weaken the system chattering, reduce the error, and improve the estimation accuracy. Therefore, the robust control method can ensure safety performance in the presence of uncertain model and uncertain disturbances using NN. The proposed

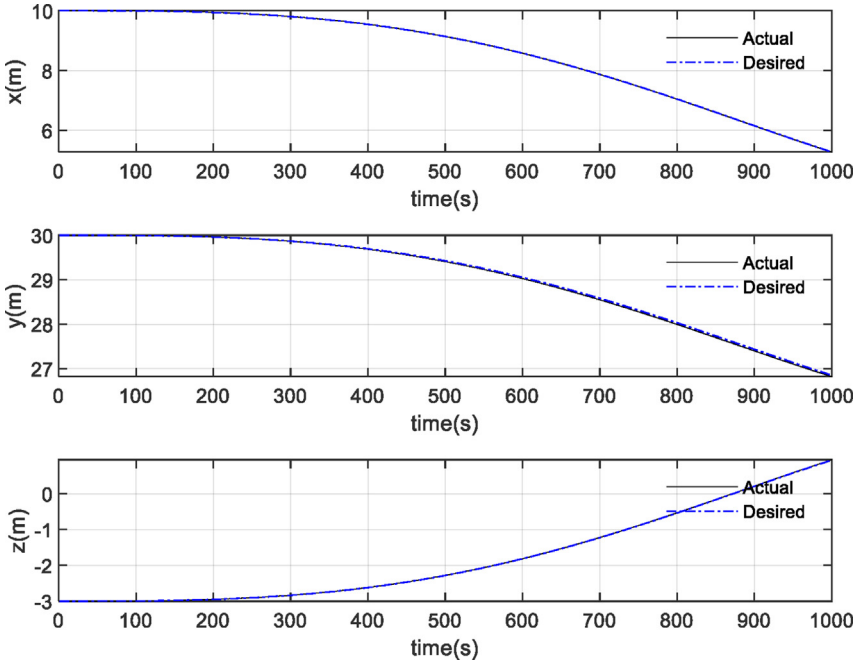

Fig. 4. Surge position, sway position, and heave position.

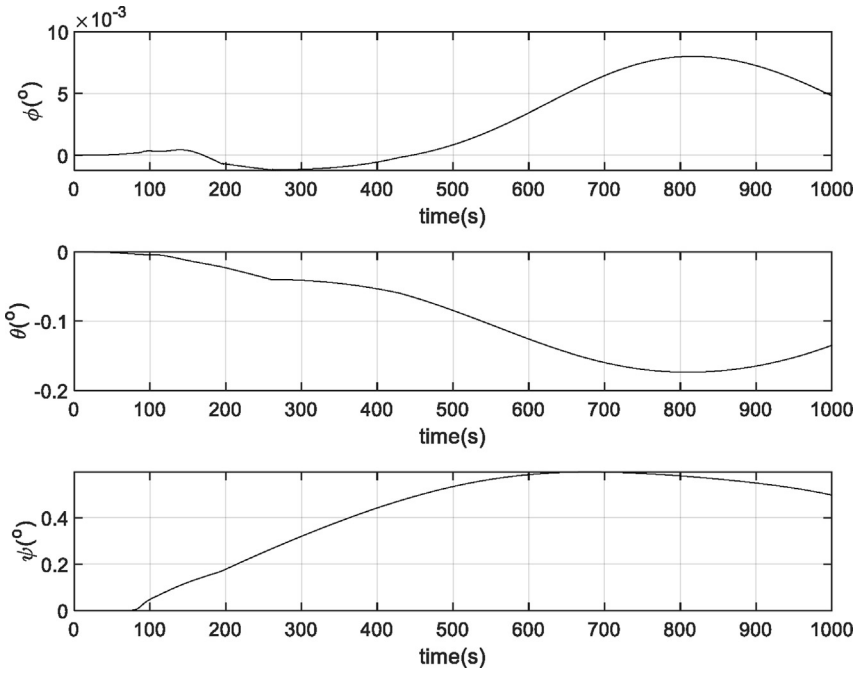

Fig. 5. Roll angle, pitch angle, and yaw angle.

algorithm convergence is proved by Lyapunov theory (*i.e.*, it is proved to converge from the initial value to balance position). Finally, as it can appear, the controller ensures the tracking performance.

4.3. Discussion

The results show that the system is stable. It has superior control response performance and it is illustrated, from the tracking curve, that the new robust control can converge faster when system disturbances are present. Meanwhile, the new control algorithm has higher control accuracy and better robustness. Finally, the new algorithm ensures that the ship can reach the expected course in a shorter time.

Moreover, this new algorithm has a smaller overshoot and a shorter system adjustment time. In terms

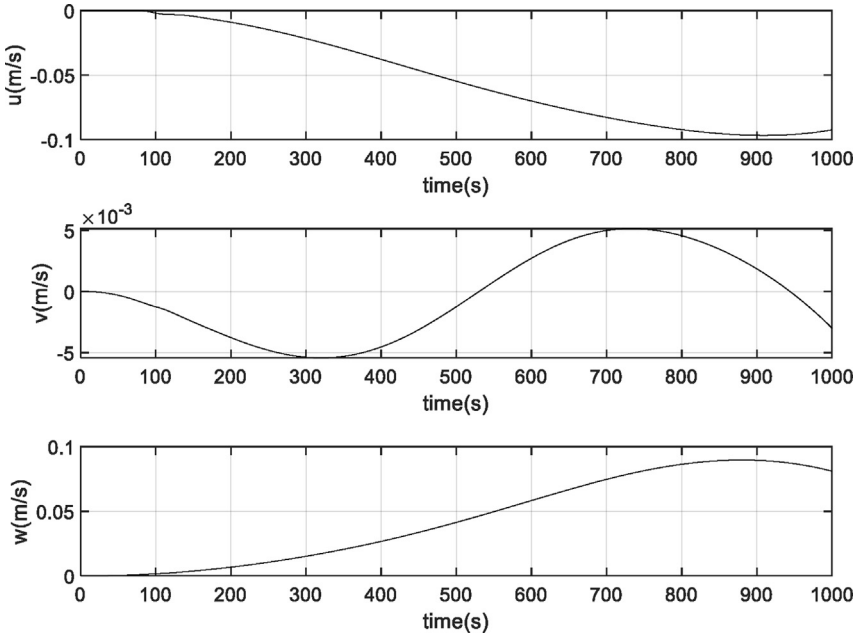

Fig. 6. Surge velocity, sway velocity, and heave velocity.

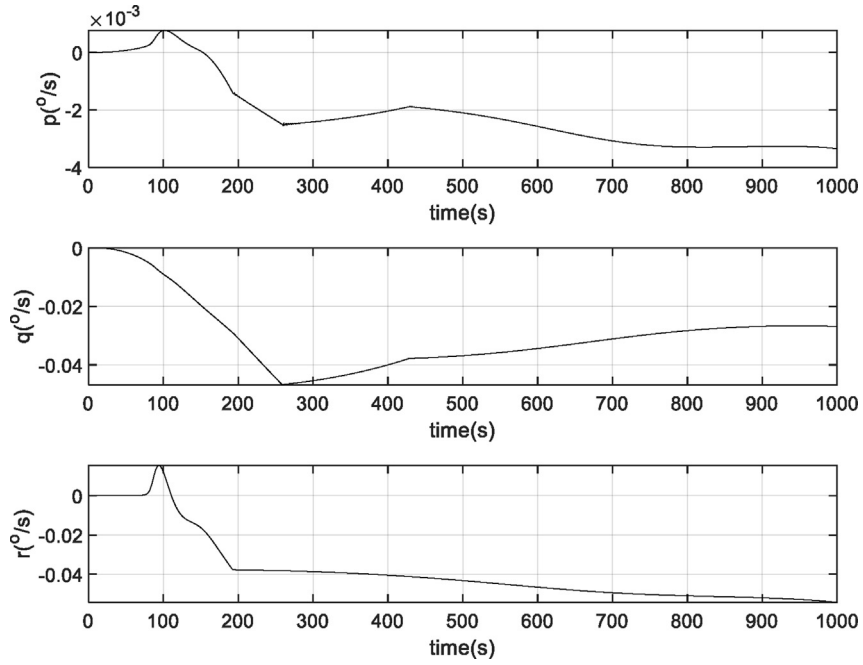

Fig. 7. Roll angle velocity, pitch angle velocity and yaw angle velocity.

of the outcomes, the results showcase its enhanced resistance to interference in unfavorable sea conditions, improved durability, and a more streamlined design. Therefore, the new fixed time sliding mode improves the convergence speed as well as the tracking error. Its tracking error dynamic equation is convergent in the case of large error and disturbance. Referring to the results shown in the above figures, the ship can fully and stably track the predefined trajectory and the system does not violate the asymmetric state constraint at all running times.

Furthermore, asymptotically convergent controllers have slow convergence speed, while finite-time convergent controllers are affected by the initial state of the system. As for the fixed time convergent controllers, they are too conservative in estimating convergence time and require cumbersome parameter calculations [33]. In view of this, this article provides a predefined time control method based on preset performance.

With the progress and development of modern industry, the design of control algorithms for several industrial applications need to meet certain time response constraints for safety standards. For example, ship motion needs to achieve ideal control accuracy in a short and fixed time. Alternatively, an unmanned ship needs to arrive at the desired location within the specified time. Therefore, based on the above discussion, it is urgent to develop a generalized, robust, and mature predefined time

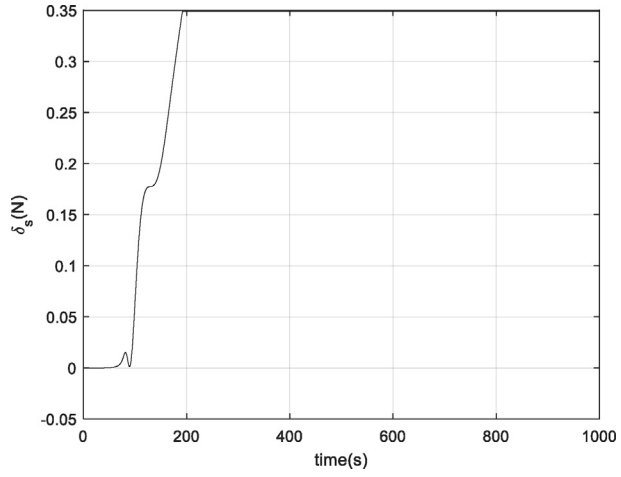

Fig. 8. Input force along the port and the starboard stern plane.

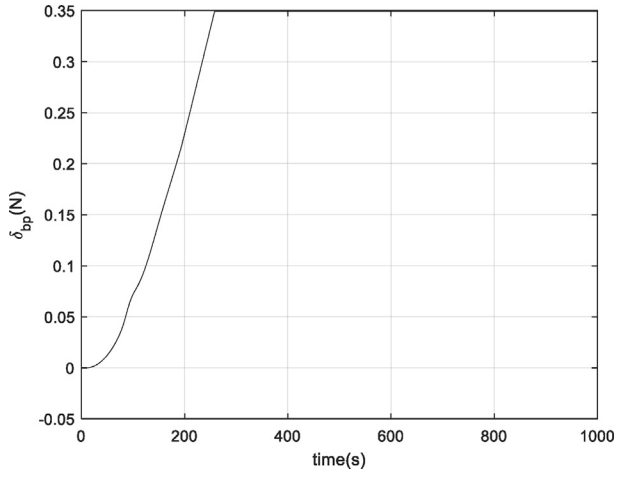

Fig. 9. Input force along the port bow plane.

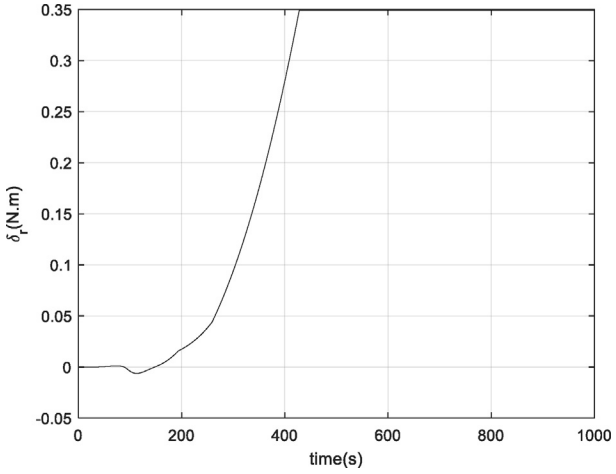

Fig. 10. Torque by the top and bottom stern rudder.

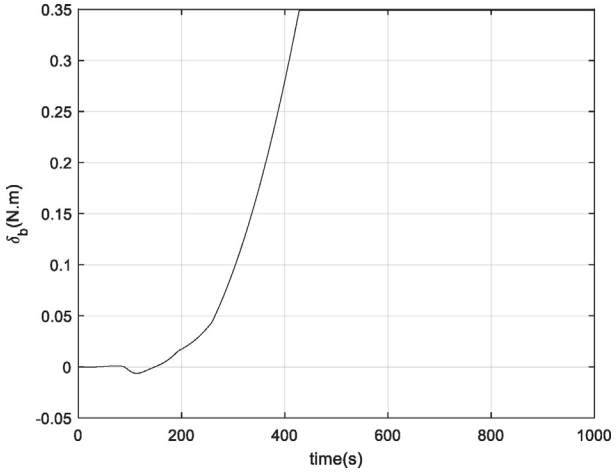

Fig. 11. Torque by the top and bottom bow rudder.

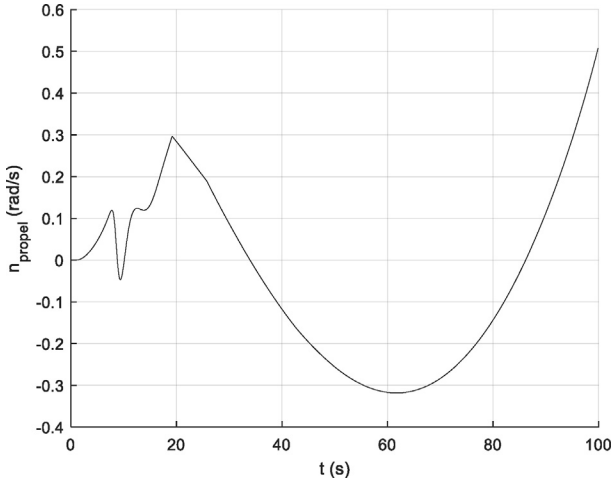

Fig. 12. Rotation speed of the propeller.

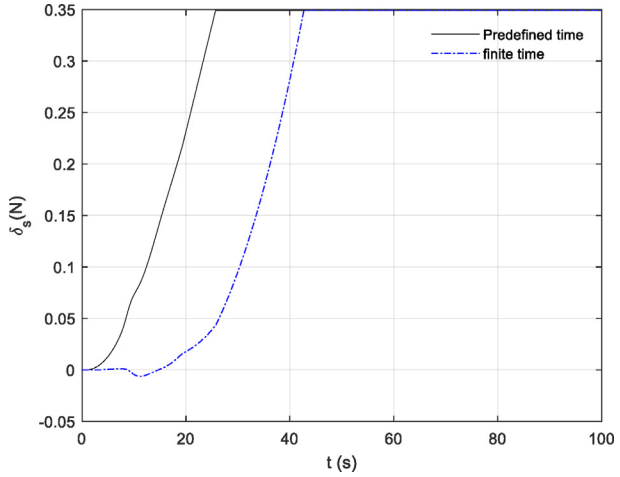

Fig. 13. Comparison between the input force δ_s.

control theory system for uncertain nonlinear systems, and to apply it to practical engineering systems. These are possible application scenarios of the proposed algorithm.

At present, there are still several issues related to predefined time control that must be further addressed. A summary of such problems that can be further discussed are listed below. First, this paper does not consider the event triggering strategy, and the way to achieve predefined time stability and save communication resources, under the event triggering strategy, is a topic worth further exploration. Second, this article investigates the problem of predefined time intelligent tracking control considering that the controlled system state is measurable. However, in practical systems, there are lots of situations where the state cannot be measured. Therefore, observer-based predefined time intelligent control is also an interesting topic to tackle.

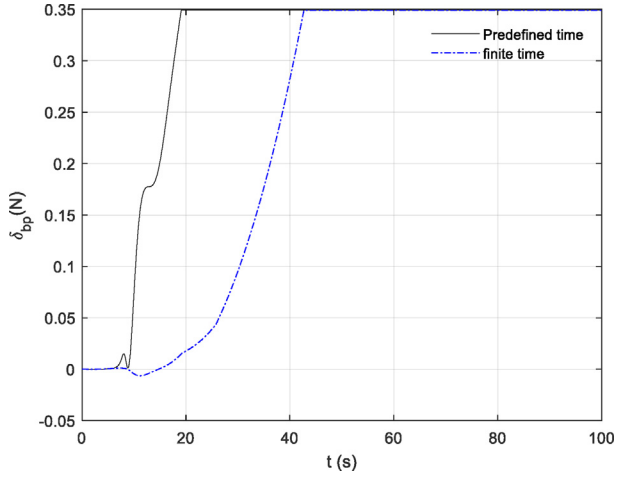

Fig. 14. Comparison of input force δ_{bp}.

5. Conclusion

In this study, a novel predefined-time sliding mode control is designed. The control approach is keen to converge from the initial value to a balance position based on the Jensen's inequality. Moreover, it is proven that the convergence from the initial value to balance position is feasible. The proposed control method can deal with ship motion system having six DOF and exposed to external disturbance and parameter's uncertainty. A designed NN suppresses the adverse effects of interference on the system. Therefore, the control method is more suitable for practical application as the controller ensures the stability of the system state in the presence of uncertain model and uncertain disturbances. Moreover, it is illustrated from the obtained results that the system can deal with unknown disturbances, ensure the safe navigation, and keep the good tracking of the route under difficult environmental conditions. As for the proposed algorithm with predefined-time convergence, it is more suitable for practical application as it achieves high precision, high speed disturbance observation, and trajectory tracking control. To sum up, the proposed algorithm can improve the convergence speed, the weaken system chattering as well as reduce the errors and improve estimation accuracy.

In engineering applications, to run the controlled system efficiently, it is often necessary to adjust the control parameters online in order to meet the actual needs and applications. The way to adjust the system control parameters adaptively is the next step of future research. Moreover, observer based on predefined time intelligent control, is also further research work. In future, the event triggering strategy will be studied. Moreover, we will interfere with the more common winds and waves in navigation.

Conflict of interest

The author declares that they have no conflicts of interest in the research presented in this manuscript.

Acknowledgement

This work was supported in part by the National Natural Science Foundation of China (No. 52201411) and Natural Science Foundation of Fujian Province (No. 2021J01819).

Appendix

The abbreviations and meaning of variables in main content are listed in Table 1.

Table 1. Nomenclature

Symbol	Quantity
R	rotation matrix
τ	input force and moment
λ	parameter
d	disturbance
e	filtering error
V	Lyapunov function
h	Radial basis function
μ	center vector of hidden layer neurons
σ	width of the radial basis function
φ	approximation error
W	weight matrix
$\tilde{W}$	error of W
$\widehat{W}$	estimation of W
τ_d	disturbance and uncertain model
τ_1	disturbance
$\tilde{\tau}_d$	estimation error of the disturbance
$\widehat{\tau}_d$	estimation of τ
ε	approaching error
J	transformation matrix
C_1	Coriolis and Centripetal torques matrix
M_1	manipulator inertial mass matrix
g	generalized gravitational and buoyancy forces
g_0	Static restoring forces and moments due to ballast systems and water tanks
D_1	linear hydrodynamic damping parameter matrix
n	propeller's speed of rotation
δ_s	force along the port and starboard stern plane
δ_{bp}	force along the port bow plane
δ_{bs}	force along the starboard bow plane
δ_r	torque by the top and bottom stern rudder
δ_b	torque by the top and bottom bow rudder
η	position and attitude of ship
ν	velocity vector
u	surge velocity
v	sway velocity
w	heave velocity
p	roll velocity
q	pitch velocity
r	yaw angle velocity
x	surge position
y	sway position
z	heave position
ϕ	roll angle
θ	pitch angle
ψ	yaw angle
α	exponent
β	exponent
m	exponent
s	sliding mode surface
I	identity matrix
k	gain
c	parameter
d	parameter
M	nominal weight inertia and hydrodynamic additional inertia
D	nominal linear hydrodynamic damping parameter matrix
C	nominal Coriolis and Centripetal torques matrix
η_d	desired trajectory
$\tilde{\eta}$	tracking error of the trajectory
$\widehat{\tau}_d$	estimated disturbance and uncertain model of τ_d

(*continued on next page*)

Table 1. (continued)

Symbol	Quantity
a	exponent
f	convex function
g	convex function
n	dimension of vector
T	time
T_2	convergence time
$\triangle M$	modelling uncertainty of M
$\triangle C$	modelling uncertainty of C
$\triangle D$	modelling uncertainty of D
f_2	continuously differentiable function
LPV	Linear parameter varying
DOF	degree-of-freedom

References

[1] Zhao LM, Roh MI, Lee SJ. Control method for path following and collision avoidance of autonomous ship based on deep reinforcement learning. Journal of Marine Science and Technology-Taiwan 2019;27(4):293−310.

[2] Lisowski J. Dynamic games methods in synthesis of safe ship control algorithms. J Adv Transport 2018;2018. https://doi.org/10.1155/2018/7586496. Art. no. 7586496.

[3] Sun Q, Chen J, Yu W, Su H. Fuzzy-sliding-mode-based robust tracking control of autonomous underwater vehicles. J Mar Sci Technol 2020;28(2). https://doi.org/10.6119/JMST.202004_28(2).0002. Article 2.

[4] Liang CD, M, Ge F, Liu ZW, Ling G, Liu F. Predefined-time formation tracking control of networked marine surface vehicles. Control Eng Pract 2021;107. Art. no. 104682.

[5] Souissi S, Boukattaya M. Time-varying nonsingular terminal sliding mode control of autonomous surface vehicle with predefined convergence time. Ocean Eng 2022;263. Art. no. 112264.

[6] Yang Y, Ge M, Liang C, Xu K, Wang L. Predefined-time formation control of NASVs with fully discontinuous communication: A novel hierarchical event-triggered scheme. Ocean Eng 2023;268. Art. no. 113422.

[7] Wang Y, Wang Z, Chen M, Kong L. Predefined-time sliding mode formation control for multiple autonomous underwater vehicles with uncertainties. Chaos, Solit Fractals 2021;144. Art. no. 110680.

[8] Mazhar N, Mumtaz F, AbidRaza M, Khan R. Predefined-time control of nonlinear systems: A sigmoid function based sliding manifold design approach. Alex Eng J Sep. 2022;61(9):6831−41.

[9] Xu S, Guan Y, Bai Y, Wei C. Practical predefined-time barrier function-based adaptive sliding mode control for reusable launch vehicle. Acta Astronaut Mar. 2023;204:376−88.

[10] Ju X, Wei C, Xu H, Wang F. Fractional-order sliding mode control with a predefined-time observer for VTVL reusable launch vehicles under actuator faults and saturation constraints. ISA (Instrum Soc Am) Trans Oct. 2022;129:55−72. Part B.

[11] Liang C-D, Ge M-F, Liu Z-W, Wang L, Park JH. Model-free cluster formation control of NMSVs with bounded inputs: A predefined-time estimator-based approach. IEEE Transactions on Intelligent Vehicles 2022. https://doi.org/10.1109/TIV.2022.3182992.

[12] Liu Y, Yan W, Zhang T, Yu C, Tu H. Trajectory tracking for a dual-arm free-floating space robot with a class of general nonsingular predefined-time terminal sliding mode. IEEE Transactions on Systems, Man, and Cybernetics: Systems May 2022;52(5):3273−86.

[13] Sun Y, Gao Y, Zhao Y, Liu Z, Wang J, Kuang J, Yan F, Liu J. Neural network-based tracking control of uncertain robotic systems: Predefined-time nonsingular terminal sliding-mode approach. IEEE Trans Ind Electron Oct. 2022;69(10):10510−20.

[14] Ferrara A, Incremona GP. Predefined-time output stabilization With second order sliding mode generation. IEEE Trans Automat Control Mar. 2021;66(3):1445−51.

[15] Huang S, Wang J, Xiong L, Liu J, Li P, Wang Z. Distributed predefined-time fractional-order sliding mode control for power system with prescribed tracking performance. IEEE Trans Power Syst May 2022;37(3):2233−46.

[16] Shao K, Zheng J. Predefined-time sliding mode control with prescribed convergent region. IEEE/CAA Journal of Automatica Sinica May 2022;9(5):934−6.

[17] Tang R, Shao K, Liang B, Xu F. Trigonometric-type sliding mode control with exact convergence time. IEEE Control Systems Letters 2022;6:2389−94.

[18] Yu G, Li Z, Liu H, Zhu Q. Predefined time nonsingular fast terminal sliding mode control for trajectory tracking of ROVs. IEEE Access 2022;10:107864−76.

[19] Huang S, Xiong L, Zhou Y, Liu J, Jia Q, Li P, Wang J. A novel distributed predefined-time sliding mode controller for performance enhancement of power system under input saturation. IEEE Transactions on Circuits and Systems I: Regular Papers Oct. 2022;69(10):4284−97.

[20] Tao M, Liu X, Shao S, Cao J. Predefined-time bipartite consensus of networked Euler-Lagrange systems via sliding-mode control. IEEE Transactions on Circuits and Systems II: Express Briefs Dec. 2022;69(12):4989−93.

[21] Ma H, Liu W, Xiong Z, Li Y, Liu Z, Sun Y. Predefined-time barrier function adaptive sliding-mode control and its application to piezoelectric actuators. IEEE Trans Ind Inf Dec. 2022;18(12):8682−91.

[22] Li Q, Yue C. Predefined-time polynomial-function-based synchronization of chaotic systems via a novel sliding mode control. IEEE Access 2020;8:162149−62.

[23] Liang C, Ge M, Liu Z, Zhan X, Park JH. Predefined-time stabilization of T−S fuzzy systems: A novel integral sliding mode-based approach. IEEE Trans Fuzzy Syst Oct. 2022;30(10):4423−33.

[24] Ni JK, Shi P. Global predefined time and accuracy adaptive neural network control for uncertain strict-feedback systems with output constraint and dead zone. IEEE Transactions on Systems, Man, and Cybernetics: Systems 2020;99:1−16.

[25] Fossen TI. Handbook of marine craft hydrodynamics and motion control. Wiley (John Wiley and Sons): Hoboken, New Jersey, USA; 2011.

[26] Ye J, Roy S, Godjevac M, Baldi S. A Switching Control Perspective on the Offshore Construction Scenario of Heavy-Lift Vessels. IEEE Trans Control Syst Technol Jan. 2021;29(1):470−7. https://doi.org/10.1109/TCST.2020.2978446.

[27] Ye J, Roy S, Godjevac M, Reppa V, Baldi S. Robustifying Dynamic Positioning of Crane Vessels for Heavy Lifting Operation. IEEE/CAA Journal of Automatica Sinica April 2021;8(4):753−65. https://doi.org/10.1109/JAS.2021.1003913.

[28] Ye J, Roy S, Godjevac M, Baldi S. Observer-based robust control for dynamic positioning of large-scale heavy lift vessels. IFAC-PapersOnLine 2019;52(3):138−43.

[29] Torres JDS, Gutiérrez DG, López E, Loukianov AG. A class of predefined-time stable dynamical systems. IMA J Math Control Inf 2017;32:1−29.

[30] Rodríguez EJ, Torres JDS, Gutiérrez DG, Loukianov AG. Predefined-time backstepping control for tracking a class of mechanical systems. IFAC-PapersOnLine 2017;50(1):1680−5.

[31] Fossen TI. Guidance and control of ocean vehicles. England: John Wiley and Sons Ltd; 1994.

[32] Huang Y, Jia Y. Adaptive finite time distributed 6-DOF synchronization control for spacecraft formation without velocity measurement. Nonlinear Dynam 2019;95(3):2275−91.

[33] Xue H, Ou Y. A Novel Asymmetric Barrier Lyapunov Function-based Fixed-time Ship Berthing Control Under Multiple State Constraints. Ocean Eng 1 August 2023;281. https://doi.org/10.1016/j.oceaneng.2023.114756. Art. no. 114756.